PHYSICAL REVIEW B VOLUME 26, NUMBER 4 15 AUGUST 1982

Theory of metal—ionic-insulator interfaces

T. E. Feuchtwang,* D. Paudyal, and W. Pong
Department of Physics and Astronomy, University of Hawaii, Honolulu, Hawaii 96822
(Received 22 March 1982)

A theory of the interfacial dipole energy and the threshold for photoemission from metals covered with a thin layer of ionic insulator was developed. The calculated thresholds are found to be in good agreement with recent measured values for metal-BaF_2 and metal-LiF systems. Moreover, the calculations agree with the observed interface parameter S, the systematic dependence of the thresholds on the insulator, and the observation that the thresholds tend to be smaller than the metal work function. The model includes a multiband free-electron description of the metal and a two-band model of the ionic insulator. The multiband feature was required for the agreement between theory and experiment, which suggests the sensitivity of the observed thresholds to band-structure effects in the metal. We also found the results to be sensitive to the choice of electron effective mass in the insulator.

I. INTRODUCTION

Because of the important applications of Schottky barriers in solid-state devices, extensive studies of Schottky-barrier formation have been made in recent years. Of particular interest in these studies is the interfacial barrier height ϕ_B of a metal-semiconductor contact. This barrier height is the difference in energy between the metal Fermi level and the bottom of the conduction band of the semiconductor. Numerous experiments have shown a linear dependence of ϕ_B on the metal electronegativity X_m.[1] The slope $(d\phi_B/dX_m)$ of this linear relationship is called the interface parameter S. An important property of S is that it indicates the extent to which the Fermi level can be stabilized for a given semiconductor. It has been established that S is small ($S \simeq 0$) for Schottky barriers involving covalent semiconductors of small band gaps.[1] For these semiconductors, the Fermi level is pinned somewhere in the band gap. It has also been found that S increases with the ionicity of the semiconductor.[1] Some recent data on S values for metal—ionic-insulator interfaces seem to indicate that the upper limit of S is about 1.6.[2] Considerable attention has been given to the theories concerning the limits of S, but some fundamental questions still remain unresolved.

Various theories have been proposed to account for pinning of the Fermi level, i.e., $S \simeq 0$.[3–12] The first qualitative explanation for $S \simeq 0$ is the Bardeen model which assumes a high density of intrinsic surface states in the gap of the semiconductor.[3] The electrons occupying these states can pin the Fermi level and screen the semiconductor from the effect of the metal work function. On the other hand, Heine[4] pointed out that true surface states cannot exist at the interface between a metal and a semiconductor. He suggested that metal-induced states in the gap of the semiconductor which decay exponentially into the semiconductor could stabilize the Fermi level. More recently, Louie *et al.*[10] proposed a new type of metal-induced gap states which can be interpreted as surface states matched to the continuum states of the metal. Using a model involving these states, they were able to explain quantitatively the variation of ϕ_B for the different metal-semiconductor interfaces. However, some questions about the application of the model of metal-induced states have been raised. For extended bulk metal states to occur the metal film has to be sufficiently thick, but it has been observed recently that the Fermi-level pinning can take place long before a sufficiently thick metal film has been deposited on the semiconductor surface.[13] In an effort to account for this observation, Spicer *et al.*[12] suggested the possibility of Schottky-barrier formation due to defects produced near the interface by metal deposition or by oxidation. Thus there is disagreement on the theoretical approach to explain the Fermi-level pinning in Schottky barriers.

In this paper we focus our attention on the interfacial barrier between a metal and a thin film of

ionic insulator and its relation to the upper limit of S. In a recent photoemission study, metal films with thin overlayers of BaF_2 or LiF were found to have photoemission thresholds lower than the corresponding metal-vacuum work function.[2] The observed difference is probably caused by the change in dipole energy of the interface. However, it is not clear from the current theories how the decrease in threshold can be predicted. The first objective of the present work has been to develop a relatively simple model involving metal-induced interfacial states to calculate the change in threshold of photoemission from a metal with a thin overlayer of ionic insulator. A second objective was to obtain a further quantitative corroboration for the validity of models involving metal-induced interfacial states.

In our model of the metal-insulator interface, we used a multiband free-electron model for the metal[14] and a two-band model of the ionic insulator.[15–17] We devised a self-consistent iterative process to calculate the interfacial dipole energy and the photoemission threshold. The theory was applied to eight metal-BaF_2 and eight metal-LiF interfaces. The agreement with the recent experimental results[2] is remarkable, and tends to confirm the concept of metal-induced interfacial states proposed by Heine[4] and Louie *et al.*[8,10]

In Sec. II we describe a simple model for the change in the surface dipole energy of a metal due to the overlayer of an ionic insulator. The method of calculating the photoemission threshold of the metal with a thin ionic insulator is discussed in Sec. III. A comparison of the results of calculations with the experimental data is given in Sec. IV. A discussion of the relation of the present work to the published work using the static dipole model is given in Sec. V. The concluding remarks are found in Sec. VI. The working expressions actually used to evaluate the interfacial dipole energies are discussed in Appendixes A and B.

II. THE MODEL

A. Preliminary remarks

In this section we introduce a modified multiband free-electron model for the semi-infinite metal. The model includes, in a phenomenological fashion, both an exchange and correlation correction as well as the gross effects of the periodic potential, i.e., of the band structure, on the density of states.

Exchange and correlation effects are accounted for in the definition of the effective one-electron surface barrier height at the metal-vacuum interface, in terms of the observed work function of the metal surface and Fermi energy. Furthermore, the surface- or interface-induced inhomogeneity of the charge density is screened by the (self-consistent-field) dielectric response function of the electron gas.[18] Band-structure effects are included in the multiband free-electron model by representing both the dispersion relation and the density of states as superpositions of several, possibly orbitally degenerate, free-electron bands starting at prominent band edge determined either from experimental data, or from calculated band structures.[14]

The multiband free-electron model is combined with a two-band model of the insulator to obtain a model of the metal-insulator interface.[15–17] Our model characterizes the interface by the parameters Δ_0 and Δ_1 representing, respectively, the contribution of the interfacial electric dipole moments to the threshold energy for photoemission from the metal into vacuum without and with an insulating film. More precisely, the shift in the photoemission threshold due to the insulating film is $(\Delta_1-\Delta_0)$. For the metal-insulator interface our model indicates that this energy is linearly related to the shift in the location of the surface Fermi level relative to the bottom of the conduction band of the insulator, i.e., to the conventional metal-insulator barrier ϕ_B. The dipole energies Δ_0 and Δ_1 are defined by a set of equations, which have to be solved numerically by an iterative procedure discussed in Sec. III. It should be noted that the effects of localized states due to bulk doping or lattice defects in the insulator are not considered. This approach can be justified by the small penetration depth (of the order of 1 Å) and high density of the metal-induced (interfacial) states considered in our work. A similar procedure was applied by Garcia-Moliner *et al.*[17] in their discussion of semiconductor surfaces.

B. The model of the metal-vacuum interface

We shall consider first the single-band model, applicable to alkali metals. In this model we represent the metal by a semi-infinite free-electron model with a finite surface barrier, located at $z=0$, of height $E_{\rm cm}$ given by

$$E_{\rm cm}=E_F+\phi_{\rm mv}\ , \tag{2.1a}$$

where E_F is the Fermi energy and $\phi_{\rm mv}$ is the mea-

sured metal-vacuum work function for a polyscrystalline film. The energy Δ_0 represents the interfacial dipole energy associated with the metal-vacuum interface. Accordingly we write

$$\phi_{\rm mv}=\phi_{\rm mb}+\Delta_0 , \tag{2.1b}$$

where $\phi_{\rm mb}$ is the bulk contribution to the work function, or the "internal" work function. We can calculate Δ_0 from empirical parameters, using the model presented in Fig. 1.

1. *Dipole energy* Δ_0

The dipole energy Δ_0 is the sum of two terms. The first is due to the dipole moment of the charge transferred across the fiducial surface plane at $z=0$. The second term is due to the charge deficiency per unit area, $e\eta_0$, centered at the screened penetration depth δ_m. Using the occupied single-electron wave functions $\Psi_n(r)$ to describe the number density, we can write

$$\Delta_0= -4\pi e^2 \int_{-\infty}^{0} \sum_n{}' \,|\Psi_n|^2 z\, dz + 4\pi e^2 \delta_m \int_{-\infty}^{0} \sum_n{}' \,|\Psi_n|^2 dz , \tag{2.2}$$

where the summation over n includes only occupied states. The wave function $\Psi_n(\vec{r})$ is given by

$$\Psi_n(\vec{r})=A^{-1/2} e^{i\vec{k}_\rho\cdot\vec{\rho}}\psi_{\vec{k}_\rho,E}(z) , \tag{2.3}$$

where the z-dependent factor of the wave function $\psi_{\vec{k}_\rho,E}(z)$ satisfies the one-dimensional Schrödinger equation,

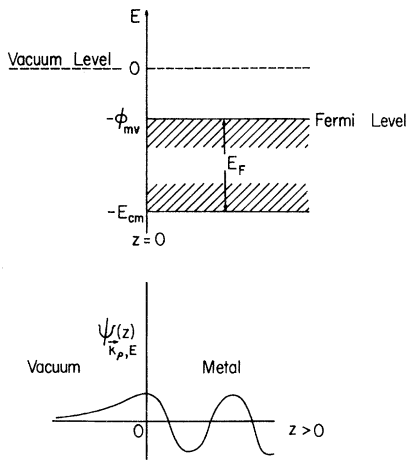

FIG. 1. Model of the metal-vacuum interface.

$$\left[-\frac{\hbar^2}{2m}\frac{d^2}{dz^2}-\left[(E+E_{\rm cm})-\frac{\hbar^2}{2m}k_\rho^2\right]\right]\psi_{\vec{k}_\rho,E}=0 , \quad z>0 \tag{2.4a}$$

$$\left[-\frac{\hbar^2}{2m}\frac{d^2}{dz^2}-\left[E-\frac{\hbar^2}{2m}k_\rho^2\right]\right]\psi_{\vec{k}_\rho,E}=0 , \quad z<0 . \tag{2.4b}$$

The energy E is assumed to be in the range

$$-E_{\rm cm}<E<0 .$$

The solutions of (2.4a) and (2.4b) are

$$\psi_{\vec{k}_\rho,E}(z)=(e^{-ikz}+{\rm Re}^{ikz}), \quad z\geq 0 \tag{2.5a}$$

$$\psi_{\vec{k}_\rho,E}(z)=Te^{Kz}, \quad z\leq 0 \tag{2.5b}$$

where

$$k=[2m/\hbar^2)(E+E_{\rm cm})-k_\rho^2]^{1/2} , \tag{2.6a}$$

$$K=[-(2mE/\hbar^2)+k_\rho^2]^{1/2} , \tag{2.6b}$$

and

$$T=2k/(k+iK) . \tag{2.7}$$

It should be noted that the interface is assumed to be the xy plane, and periodic boundary conditions are imposed on the x and y dependence of Ψ over an area A. The two-dimensional wave vector $\vec{k}_\rho$ is given by $\vec{k}_\rho=\vec{1}_x k_x+\vec{1}_y k_y$. The two-dimensional vector $\vec{\rho}$ is $\vec{1}_x x+\vec{1}_y y$.

The screened-charge penetration depth δ_m in Eq. (2.2) is given by

$$\delta_m=z_m/\epsilon_m(q_s) , \tag{2.8}$$

where z_m is the unscreened distance from the planar interface to the center of the charge deficiency; $\epsilon_m(q_s)$ is the static longitudinal dielectric function of the metal and q_s is the wave vector of the dominant fluctuation of the screening charge. We shall use the self-consistent-field (SCF) approximation[18,19] of Lindhard to describe ϵ_m. In the SCF approximation, the electron gas exhibits an oscillatory response whose amplitude decreases with an inverse power of the distance. Thus q_s in Eq. (2.8) is the wave vector of these Friedel oscillations,[20] which is twice the Fermi wave vector k_F. It can be shown that in this approximation z_m may be taken to be a quarter of the wavelength of the Friedel oscillations.[21] Thus we have

$$z_m=\pi/4k_F , \tag{2.9}$$

and hence we write

$$\delta_m = \pi[4k_F \epsilon_{\mathrm{SCF}}(2k_F)]^{-1} . \tag{2.10}$$

If k_F is expressed in units of Å^{-1}, then Eq. (2.10) reduces to [19(b)]

$$\delta_m = \pi(4k_F + 1.2)^{-1} , \tag{2.11}$$

in units of Å. In applying Eq. (2.11), we took k_F to be the conventional Fermi wave vector

$$k_F = (3\pi^2 N)^{1/3} , \tag{2.12}$$

where N is the number of valence electrons per unit volume. This choice implies that the screening of the charge deficiency is primarily due to the response of the essentially free s-p (valence) electrons. The screening due to the d electrons is neglected. We assume that there is considerable localization of the d electrons at the ionic cores which prevents them from contributing significantly to the screening of "external" charges.[14]

A method of calculating the dipole energy Δ_0 using Eq. (2.2) for a simple s-type conduction band is given in Appendix A. The generalization of this method to account for d electrons is also discussed in Appendix A.

2. *Additional free-electron bands*

The single-band model described above has to be generalized for all but the alkali metals. This generalization is to account for gross band-structure effects on the density of occupied states representing the p-type electrons in divalent and trivalent metals, and of the d electrons in transition metals. We shall describe these electrons by additional free-electron bands to be determined from the following general parameterization of the density of states:

$$D(E) = \sum_{\alpha} D_{\alpha}(E) , \tag{2.13}$$

where

$$D_{\alpha}(E) = \frac{g_{\alpha}}{2\pi^2}\left[\frac{2m}{\hbar^2}\right]^{3/2}\left[\frac{m_{\alpha}}{m}\right]^{3/2}(E + E_{\alpha,1})^{1/2} \times \Theta(E + E_{\alpha,1})[1 - \Theta(E + E_{\alpha})] . \tag{2.14}$$

Here α refers to the s, p, or d band. g_{α} is the orbital degeneracy of the band, i.e., in general

$$g_{\alpha} = (2l + 1) , \tag{2.15}$$

where $l = 0, 1, 2, \ldots$. An exception to this rule might occur when, as in Cr, the d bands exhibit a pronounced grouping into two subgroups of degeneracy 2 and 3 which can be interpreted as a manifestation of the lifting of the fivefold orbital degeneracy in a cubic crystal field.[22] The unit step function Θ is defined by

$$\Theta(x) = \begin{cases} 1, & x > 0 \\ 0, & x < 0 . \end{cases} \tag{2.16}$$

The parameters for the explicit representations of the densities of states, which were deduced for the metals considered in our calculations, are presented and discussed in Sec. III C. The wave functions for the p and/or d electrons are given by Eqs. (2.5)—(2.7) with the replacement of m by m_{α}, and E_{cm} by $E_{\alpha,1}$, the bottom of the lowest α band. E_{α} is either the top of the α band or the Fermi level, depending on which is lower. We note that the localization of the d electrons can be characterized by the increase in their effective mass, which suggests a reduced probability of tunneling across the surface barrier.[23]

Using Eq. (2.14), we find that the number of α electrons per unit volume N_{α} can be expressed as

$$N_{\alpha} = \frac{g_{\alpha}}{2\pi^2}(2m/\hbar^2)^{3/2}(m_{\alpha}/m)^{3/2} \times \int_{-E_{\alpha,1}}^{-E_{\alpha}} (E + E_{\alpha,1})^{1/2} dE . \tag{2.17}$$

Equation (2.17) can be applied to calculate the effective-mass ratio m_{α}/m for α bands that have the highest occupied states at E_{α}. However, for electrons in the filled d bands, the effective mass is estimated using the tight-binding approximation.

C. Model of the metal-insulator interface

We represent the semi-infinite insulator by a modified effective-mass two-band model, using the Franz interpolation to represent the complex dispersion relation. This representation is adequate over the energy interval $-E_v < E < -E_c$, corresponding to the energy gap of width E_g.[15—17] The model and the empirical parameters are shown in Fig. 2.

Proceeding as in the case of the metal, we have

$$\Psi(r) = A^{-1/2} e^{i\vec{k}_{\rho}\cdot\vec{\rho}} \psi_{\vec{k}_{\rho},E}(z) . \tag{2.18}$$

Clearly, a wave function representing an electron incident at the interface from the right ($z > 0$) with an energy falling into the forbidden gap acquires an exponentially attenuated "tail" which "fringes"

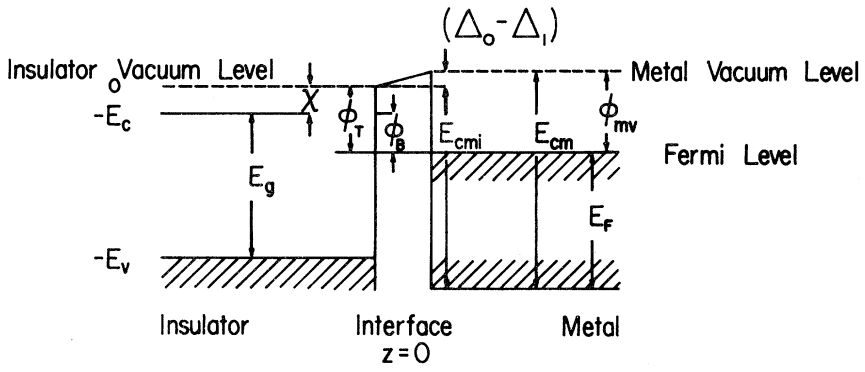

FIG. 2. Model of the metal-insulator interface.

into the barrier. Thus we write

$$\psi_{\vec{k}_\rho,E}(z)=Te^{-i(k_I+iK_I)z}, \tag{2.19}$$

where $z\leq 0$ and the smallest gap is located at $k_z=k_I$. The imaginary part of the z component of the wave vector K_I is a function of the energy, which in principle can be determined.

1. *The complex band structure of the insulator*

For our purposes, the Franz interpolation formula[16] provides an adequate representation of $K_I(E,\vec{k}_\rho)$. It is given by

$$K_I=[-(2m_I/\hbar^2)(E+E_v)(E+E_c)E_g^{-1}+(\vec{k}_\rho-\vec{k}_{\rho_0})^2]^{1/2}. \tag{2.20}$$

This formula assumes a direct gap of width E_g at $\vec{k}=\vec{k}_I$ and extending from $E=-E_v$ to $E=-E_c$. An indirect gap may in general involve an energy-dependent complex wave vector. That is, both the real and the imaginary parts of the z component of the wave vector may vary with energy over the gap.[24] However, we shall assume that $\vec{k}_I=0$ $\vec{k}_{\rho_0}=0$, and $m_I>m$. m_I is the effective mass of the electron in the valence band. The method of estimating m_I is discussed in Appendix B.

It is interesting to note that in the limit of very large gaps, Eq. (2.20) reduces to

$$K_I=\left[-\frac{2m_I}{\hbar^2}(E+E_c)+(\vec{k}_\rho-\vec{k}_{\rho_0})^2\right]^{1/2}. \tag{2.21}$$

The similarity of Eqs. (2.21) and (2.6b) is obvious, particularly when $\vec{k}_{\rho_0}=0$. This suggests the fringing of a metal state into an insulator with an infinite energy gap is quite similar to its fringing into the surface barrier across the metal-vacuum interface. However, less fringing is expected in the insulator if the electron affinity of the insulator is negative. Furthermore, we note that the maximum value of K_I occurs at midgap and is

$$(K_I)_{\max}=[(2m_I/\hbar^2)E_g/4+(\vec{k}_\rho-\vec{k}_{\rho_0})^2]^{1/2}. \tag{2.22}$$

Thus, the attenuation of the metal states in the insulator at midgap increases with the band gap E_g. We shall apply this conclusion below.

The metal-insulator interface is represented by a model derived from the models for the metal and insulator discussed above. The interface is assumed to be a plane across which both the periodic potential and dielectric constant change abruptly. The energy difference between the metal Fermi level and the vacuum level of the insulator is $\phi_B+\chi$. This energy is related to the work function $\phi_{\rm mv}$ by the following equation

$$\phi_B+\chi=\phi_{\rm mv}+\Delta_1-\Delta_0. \tag{2.23}$$

Here χ is the electron affinity of the insulator and ϕ_B is the effective barrier height from the metal Fermi level to the conduction band of the insulator as indicated in Fig. 2. The dipole energy Δ_0 is determined by Eq. (A19). Hereafter we shall distinguish corresponding quantities for the metal-vacuum and metal-insulator interfaces by subscript 0 and 1, respectively.

2. *Dipole energy Δ_1*

A simple generalization of Eq. (2.2) enables us to write an implicit equation for the dipole energy Δ_1. Summing the dipole energies of the free-electron bands, we write

$$\Delta_1=-4\pi e^2\sum_\alpha\left[\frac{1}{\epsilon_I(\bar{q}_\alpha)}\sum_n{}'\int_{-\infty}^{0}|\Psi_{n,\alpha}(\vec{r})|^2 z\,dz-\delta_m\sum_n{}'\int_{-\infty}^{0}|\Psi_{n,\alpha}(\vec{r})|^2 dz\right]. \tag{2.24}$$

The wave function $\Psi_{n,\alpha}$ is given by

$$\Psi_{n,\alpha}(\vec{r})=A^{-1/2}e^{i\vec{k}_\rho\cdot\vec{\rho}}\psi_{\vec{k}_\rho,E,\alpha}(z)\,, \tag{2.25}$$

where

$$\psi_{\vec{k}_\rho,E,\alpha}(z)=(e^{-ikz}+\mathrm{R}e^{ikz}),\quad z\geq 0\,, \tag{2.26}$$

$$\psi_{\vec{k}_\rho,E,\alpha}(z)=Te^{-i(k_I+iK_I)z},\quad z\leq 0\,. \tag{2.27}$$

In Eq. (2.24), the sum over the occupied "modified" metal states $\sum'$ is restricted to states whose energy falls into the forbidden gap of the insulator. In Eq. (2.27), the z component of the complex wave vector (k_I+iK_I) in the insulator was defined by Eqs. (2.19) and (2.20). Using the continuity conditions imposed on the effective-mass wave functions,[25,26] we find

$$T=(m_I/m_\alpha)2k[(m_I/m_\alpha)k+k_I+iK_I]^{-1}\,. \tag{2.28}$$

The dielectric function ϵ_I is the static nonlocal response of the insulator evaluated at an average screening wave vector $\bar{q}_\alpha$ to be discussed in Sec. III B.

Evidently, depending on the choice of the energy reference (at the metal or the insulator vacuum level), either k or K_I depends explicitly on the dipole energy Δ_1. It is for this reason that Eq. (2.24) is only an implicit equation for Δ_1, which has to be solved by iteration. The details of this solution are discussed in Sec. III.

At this point, it might be helpful to review the physical interpretation of Eqs. (2.24)–(2.28). As indicated by Eq. (2.25), the junction has eigenstates whose energies fall into two distinct categories, depending on whether their energies fall into allowed bands or forbidden gaps of the metal.[27] The former interfacial states are represented by Eqs. (2.25)–(2.28) and are best viewed as modified metal states, which fringe into the insulator. The latter are relatively uncommon and correspond to proper interfacial states, which are spatially localized at the interface. That is, they decay exponentially with distance from the interface, both in the metal and in the insulator. In our model the exponentially attenuated tails of the modified metal states, which fringe into the insulator, are responsible for the charge transfer from the metal to the barrier. This charge transfer gives rise to the interfacial dipole moment and the associated dipole energy $\Delta_1^{(\alpha)}$ for a given α band. Equation (2.24) indicates two distinct contributions to the interfacial dipole moment per unit area. The first is the dipole moment per unit area $e\mu_{1-}^{(\alpha)}$ of the charge transferred out of the metal relative to the nominal interface at $z=0$. The second is the moment $-ez_m\eta_{1,\alpha}$ of the electronic charge deficiency per unit area on the metal side of the interface. This charge deficiency is assumed to be screened by the dielectric response function $\epsilon_m(q_s)$, while the charge transferred into the insulator is screened by $\epsilon_I(\bar{q}_\alpha)$. The corresponding contributions to the dipole energy are

$$\Delta_1^{(\alpha)}=-4\pi e^2[1/\epsilon_I(\bar{q}_\alpha)]\mu_{1-}^{(\alpha)}+4\pi e^2\delta_m\eta_{1,\alpha}\,, \tag{2.29}$$

where δ_m is defined by Eq. (2.8).

In principle one also should consider fringing of states in the valence band of the insulator into the metal gap extending from the lowest conduction band to the core levels. However, the large width of this gap implies that the imaginary part of the z component of the wave vector in the metal will assume a large mean value. This and the relatively high localization of the valence states in the insulator should lead to a rather negligible mean penetration depth and charge transfer from the insulator into the metal. We shall therefore neglect this contribution to the interfacial dipole energy Δ_1.

Finally we note that our model does not involve any assumption concerning the doping of the insulator or the displacement, if any, of its Fermi level from its intrinsic position at midgap. In fact, the position of the Fermi level in the bulk insulator prior to the formation of the junction does not affect our calculation. This is due to the fact that our model deals only with phenomena restricted to the relatively thin interfacial region characterized by the surface Fermi level. If we assume the insulator to be intrinsic, then the shift of the surface Fermi level is $\phi_B-\frac{1}{2}E_g$.

III. DETERMINATION OF MODEL PARAMETERS

A. Preliminary remarks

In this section we shall discuss the actual evaluation of the interfacial parameters Δ_0 and Δ_1. For

the single-band model of the metal, Eq. (2.2) presents the contribution of the dipole energy Δ_0 to the metal-vacuum work function. The explicit evaluations of Eq. (2.2) and of its generalization for the multiband free-electron model, specified by Eqs. (2.13)–(2.17), are given in Appendix A.

The numerical evaluation of Δ_0 for any model of a metal does not present any particular difficulty. In contrast to Δ_0, the dipole contribution to the photoemission threshold of metal-insulator interfaces, Δ_1, is only implicitly defined by Eq. (2.24). Thus the calculation of Δ_1 requires the self-consistent, iterative solution to be discussed in this section. The reason for this can be traced to the sum over occupied (modified) metal states in Eq. (2.24). This sum involves an integration over the metal states overlapping the forbidden gap of the insulator. However, one or both of the limits of this integral depends explicitly on the unknown energy Δ_1. Thus one has to solve for Δ_1 by successive approximations. Starting with an assumed value of Δ_1, one calculates from Eq. (2.24) a new Δ_1, which is used to determine a third value of Δ_1 and so forth. In order to speed up the iterative solution of Eq. (2.24), we introduce an unessential approximation of the sum over states, which reduces it to a closed expression and eliminates the need for a numerical integration. This approximation is discussed in Appendix B.

B. Charge penetration and screening in the insulator

In our discussion of dipole energy Δ_1 in Sec. II C 2 we mentioned that the dielectric function ϵ_I of the insulator can be evaluated at an average screening wave vector $\bar{q}$. We now give a more detailed discussion of $\epsilon_I(\bar{q})$. As indicated in Eq. (2.24), we expressed the charge per unit area transferred into the insulator by

$$e\eta_1 = e\sum_{\alpha}\sum_{n}{}' \int_{-\infty}^{0} |\Psi_{n,\alpha}(\vec{r})|^2 dz = \sum_{\alpha} e\eta_{1,\alpha} . \tag{3.1}$$

If we multiply $e\eta_1$ by a mean charge penetration length $\bar{z}_1$, we may write

$$e\eta_1\bar{z}_1 = \sum_{\alpha}\bar{z}_{1,\alpha}e\eta_{1,\alpha} , \tag{3.2}$$

where $\bar{z}_{1,\alpha}$ is a mean charge penetration distance associated with the electrons of band α of the metal. The charge penetration distances $\bar{z}_{1,\alpha}$ in the insulator[28] evidently specify the scale of the spatial variation of the charge density in the insulator. The screening of the charge fluctuations over such relatively small distances is described by the wave-vector-dependent, static longitudinal dielectric response function $\epsilon(\vec{q},\omega=0)$, evaluated at an appropriate screening wave vector $\bar{q}$. We shall show how the effective dielectric screening can be represented for a given $\bar{z}_{1,\alpha}$.

Walter and Cohen[29] calculated $\epsilon(\vec{q},\omega=0)$ for several semiconductors. They found the static dielectric response to: (i) depend weakly on the orientation of $\vec{q}$; (ii) decrease monotonically with $|\vec{q}|$ from its maximum at $q=0$; (iii) tend already for moderate values of $|\vec{q}|$ to the asymptotic Thomas-Fermi-type (TF) expression

$$\epsilon(q,0)\simeq 1+(q_s/q)^2 .$$

No comparable calculations of $\epsilon(q,0)$ are available for ionic insulators, such as LiF and BaF_2, considered in this paper. We therefore followed a suggestion of Penn[30] to approximate $\epsilon(q,0)$ by an interpolation formula

$$\epsilon_I(q,0)=1+\frac{\epsilon_I(0,0)-1}{1+(q/q_s)^2} \tag{3.3}$$

which assumes the correct value for $q=0$, and which in the limit of large q tends to the Thomas-Fermi—type expression

$$\epsilon_I(q,0)\simeq 1+[\epsilon_I(0,0)-1]\left[\frac{q_s}{q}\right]^2 . \tag{3.4}$$

Again, following Penn we choose

$$q_s^2=\left[\frac{4q_{\mathrm{TF}}^2}{3}\right][\epsilon_I(0,0)-1]^{-1} , \tag{3.5}$$

where

$$q_{\mathrm{TF}}^2=4(2m_IE_w)^{1/2}/\pi a_{\mathrm{H}}\hbar . \tag{3.6}$$

Here, m_I is the effective mass of the electron in the valence band; E_w, the valence-band width of the ionic insulator; a_{H}, the bohr radius.[19(b)]

We now can calculate the dipole moment of the screened charge $\rho_t(z)$ transferred into the insulator and express it in terms of the moment of the unscreened charge $\rho_i(z)$ divided by $\epsilon_I(\bar{q},0)$. This provides us with an implicit definition of the mean screening wave vector, or alternatively of the effective dielectric screening $\epsilon_I(\bar{q},0)$ to be used in Eq. (2.24). We can express

$$\rho_t(z)=\int_{-\infty}^{\infty}\frac{\rho_i(q)}{\epsilon_I(q,0)}e^{iqz}dq/2\pi , \tag{3.7}$$

where

$$\rho_i(q)\simeq -|T|^2 e\left[\int_{-\infty}^{0} e^{2K_I z}e^{-iqz}dz - \int_0^{\infty}(2K_I)^{-1}\delta(z)\,dz\right]. \quad (3.8)$$

The first term of the approximation given by Eq. (3.8) follows from Eq. (2.27), and the second term represents the charge deficiency in the metal, assuming it is essentially localized at the interface. Substituting Eqs. (3.3) and (3.8) into Eq. (3.7), we find

$$\int_{-\infty}^{0} z\rho_t(z)\,dz=-\frac{|T|^2 e}{(2K_I)^2}(1+f/\Omega)^{-1}, \quad (3.9)$$

where

$$\Omega=1+(f+1)[1+(f+1)^{1/2}q_s/K_I]^{-1} \quad (3.10)$$

and

$$f=\epsilon_I(0,0)-1. \quad (3.11)$$

Next, we consider the dipole moment of the unscreened charge transferred into the insulator. This quantity is given by

$$\int_{-\infty}^{0} z\rho_i(z)\,dz=-\frac{|T|^2 e}{(2K_I)^2}. \quad (3.12)$$

Hence we may define the mean screening wave vector by the following implicit equation

$$1/\epsilon_I(\bar{q}_\alpha,0)=\langle(1+f/\Omega)^{-1}\rangle_\alpha. \quad (3.13)$$

Here the angle brackets denote an average over the occupied states in a given band α weighted by $(|T|/2K_I)^2$. We approximate this average by

$$1/\epsilon_I(\bar{q}_\alpha,0)\simeq(1+f\{1+(f+1)[1+(f+1)^{1/2}q_s\langle 1/K_I\rangle_\alpha]^{-1}\}^{-1})^{-1}. \quad (3.14)$$

From the definition of $\bar{z}_{1,\alpha}$ given by Eq. (3.2), we can write

$$\langle 1/2K_I\rangle_\alpha=\bar{z}_{1,\alpha}. \quad (3.15)$$

Hence, combining Eqs. (3.5), (3.14) and (3.15), we obtain

$$\epsilon_I(\bar{q}_\alpha,0)\simeq 1+f(1+\epsilon_I(0,0)\{1+[4\epsilon_I(0,0)/3f]^{1/2}2\bar{z}_{1,\alpha}q_{\mathrm{TF}}\}^{-1})^{-1}. \quad (3.16)$$

It should be noted that $\epsilon_I(\bar{q}_\alpha,0)$ is an average screening factor.

C. Calculations of interfacial dipole energies

According to the model shown in Fig. 2, the threshold ϕ_T for photoemission into the vacuum from a metal covered with a thin layer of ionic insulator is given by

$$\phi_T=\phi_{\mathrm{mv}}+\Delta_1-\Delta_0. \quad (3.17)$$

Thus ϕ_T can be determined from the calculated values of the dipole energies Δ_0 and Δ_1 for a given metal surface of work function ϕ_{mv}. The computation involves the energy parameters of the metal and insulator. In our calculations, these quantities are specified relative to the vacuum level of the insulator. Denoting the energy bottom of the metal conduction band relative to the insulator vacuum level by E_{cmi}, we write

$$E_{\mathrm{cmi}}=E_{\mathrm{cm}}+\Delta_1-\Delta_0. \quad (3.18)$$

This implies that the location of the Fermi level of the metal-insulator interface depends on $(\Delta_0-\Delta_1)$. Hence the limits of integration over the occupied states in Eq. (2.24) involve $(\Delta_0-\Delta_1)$.

However, the implicit equation for Δ_1 can be solved by an iterative process. The starting value of Δ_1 for the interation was chosen to be Δ_0, which was calculated from Eq. (A19). The use of Eq. (2.24) to find Δ_1 also requires an initial choice of $\epsilon_I(\bar{q}_\alpha)$. Applying Eqs. (B7) and (B10), we calculated the penetration depths from

$$\bar{z}_{1,\alpha}=\mu_1^{(\alpha)}/\eta_{1,\alpha}.$$

The value of $\bar{z}_{1,\alpha}$ was then used to find $\epsilon_I(\bar{q}_\alpha)$ from Eq. (3.16). The rate of convergence and the final value of Δ_1 were insensitive to the precise choice of the starting values. The process converged rapidly, and was terminated when the change in Δ_1 fell below 5%.

Since the multiband free-electron model of the metal was applied to calculate the dipole energies, it was necessary to locate the band edges below the

TABLE I. Energy-band parameters of simple metals. Energies (in eV) are relative to the Fermi level. Indicated electronic configuration of the metal atom in the solid reflects the partial occupancy of the corresponding bands due to band overlap. When two α-type bands are introduced, the higher band is denoted by a prime, α'. The subscripts 1 and 2 denote, respectively, the lowest and highest occupied state of the α band.

Metal	ϕ_{mv}^{c}	$E_F=-E_{s_1}$	$-E_{s_2}$	$-E_{s_1'}$	$-E_{s_2'}$	$-E_{p_1}$	$-E_{p_2}$	(m_p/m)	Configuration
Na	2.3	3.3							$3s$
Mg[a]	3.6	7.1	2.7	2.8	0.0	1.6	0.0	1.0	$3s^{1.5}3p^{0.5}$
Al[b]	4.2	11.3	2.3			2.9	0.0	1.0	$3s^{2}3p$

[a]Band-structure calculation by L. M. Falicov, Philos. Trans. R. Soc. London 255, 55 (1962); J. C. Kimbal, R. W. Stark, and F. M. Mueller, Phys. Rev. 162, 600 (1967).
[b]B. Segall, Phys. Rev. 124, 1797 (1961).
[c]Unless stated otherwise, all work-function data taken from D. E. Eastman, Phys. Rev. B 2, 1 (1970), and A. H. Sommer, *Photoemissive Materials* (Wiley, New York, 1968).

Fermi level in the conduction bands relative to the Fermi level. In locating the bottom of the lowest s-type conduction band E_{s1}, we either used band-structure calculations to determine E_{Γ_1} or the conventional free-electron model applied to the sp electrons. In Tables I–III, we list the energy-band parameters for the free-electron models of the metals in the metal-insulator interfaces that we have studied. These parameters were deduced from recent experimental data, whenever available, or else from band-structure calculations. The model parameters for the ionic insulators are shown in Table IV.

IV. CALCULATED RESULTS

A. Comparison of calculated and measured thresholds

We have calculated the dipole energies Δ_0 and Δ_1 as well as the photoemission threshold ϕ_T given by $(\phi_{mv}+\Delta_1-\Delta_0)$ for various metal surfaces covered with a thin film of BaF_2 or LiF. We found the calculated values to be sensitive to the values of the multiband energy parameters and the measured metal-vacuum work functions assumed in the calculation. The calculated results are compared in Table V with the corresponding measured values of ϕ_T. In most cases, the calculated values are in good agreement with the measured ones. The largest difference, which is about 21%, is found only for the Mg-insulator interfaces.

Both the calculated and measured thresholds satisfy the inequality $\phi_T<\phi_{mv}$, which within our model is equivalent to $\Delta_1<\Delta_0$. An obvious factor that would make Δ_1 less than Δ_0 is the dielectric screening of the charge transferred into the insulator. That is, Δ_1 decreases with increasing $\epsilon_I(\bar{q}_\alpha)$. Another contributing factor is the decrease in the number of electrons transferred per unit area (η_1) from the metal into the insulator. The calculations indicate that η_1 is less than η_0.

B. Comparison of calculated and measured interface parameters

In the Introduction we mentioned that the observed Schottky-barrier height ϕ_B can be expressed as a linear function of the metal electronegativity X_m. This relationship is given by

TABLE II. Energy-band parameters of Cr. Energies (in eV) are stated relative to the Fermi level. d bands are split into a lower twofold degenerate band of e_g symmetry and a higher threefold degenerate band denoted d', of t symmetry. Subscripts 1 and 2 denote, respectively, the lowest and highest occupied states of the α band.

Metal	ϕ_{mv}	$E_F=-E_{s_1}$	$-E_{s_2}$	$-E_{d_1}$	$-E_{d_2}$	$(m_d/m)^b$	$-E_{d_1'}$	$-E_{d_2'}$	$(m_{d'}/m)^b$	Configuration
Cr[a]	3.9	7.0	0.0	4.3	0.7	1.6	1.4	0.0	1.6	$3d^5 4s$

[a]Band-structure calculation by S. Asano and J. Yamashita, J. Phys. Soc. Jpn. 23, 714 (1967).
[b]Effective mass of both d subbands was calculated using Eq. (2.17) and assuming a fivefold degenerate band.

TABLE III. Energy band parameters of noble metals. Energies (in eV) are stated relative to the Fermi level. Electronic configuration of the metal atom in the solid is listed. Subscripts 1 and 2 denote, respectively, the lowest and highest occupied state of the α band.

Metal	ϕ_{mv}^{c}	$E_F=-E_{s_1}$	$-E_{p_1}$	$-E_{s_2},-E_{p_2}$	$-E_{d_1}$	$-E_{d_2}$	(m_d/m)	Configuration
Cu[a]	4.4	7.0	3.0	0.0	5.1	2.1	1.6	$3d^{9.2}4s^{0.9}4p^{0.9}$
Ag[a]	4.0	5.5		0.0	7.1	3.6	1.1	$4d^{10}5s$
Pt[a]	5.3	6.0		0.0	6.5	0.0	1.3	$5d^{9}6s$
Au[b]	5.1	5.5		0.0	7.7	2.0	1.0	$5d^{10}6s$

[a]X-ray photoemission data by Y. Baer, P. F. Heden, I. Hedman, M. Klasson, C. Nordling, and K. Siegbahn, Phys. Scrip. 1, 55 (1970).
[b]D. E. Eastman, in *Electron Spectroscopy*, edited by D. A. Shirley (North-Holland, Amsterdam, 1972), p. 487.
[c]Unless stated otherwise, all work functions taken from D. E. Eastman, Phys. Rev. B 2, 1 (1970); and A. H. Sommer, *Photoemissive Materials* (Wiley, New York, 1968).

$$\phi_B = SX_m + \phi_0 , \tag{4.1}$$

where S is called the interface parameter. Both S and ϕ_0 are constants depending only on the insulator. Since $\phi_T = \phi_B + \chi$, we note that

$$S = \frac{\partial \phi_B}{\partial X_m} = \frac{\partial \phi_T}{\partial X_m} . \tag{4.2}$$

In Fig. 3, we present plots of the calculated ϕ_T vs X_m for metal-BaF_2 and metal-LiF interfaces. The dependence of ϕ_T on X_m is reasonably linear and the slopes of the linear fits to the calculated ϕ_T values are in good agreement with the observed S values. This agreement is all the more remarkable since it was achieved without invoking the linear dependence[31] of the work function on the metal electronegativity as indicated by

$$\phi_{mv} = AX_m + B . \tag{4.3}$$

Thus our value of S is not affected by the uncertainty in the precise value of A which in previous analyses has been assumed to range from 2 to 3.[33]

According to the static dipole model developed by Louie *et al.*,[10] the parameter S can be calculated from

$$S = \frac{A}{(1+4\pi e^2 D_s \delta_{\text{eff}})} , \tag{4.4}$$

where e is the electron charge, D_s, the density of interface states, δ_{eff}, the effective distance between the negative charge transferred to the insulator due to the change in ϕ_B and the consequent charge deficiency in the metal, and A is defined by Eq. (4.3). Equation (4.4) has recently been used to estimate the S value for large band-gap solids.[34] A value of 1.5, obtained using $A=2.3$, is in close agreement with our calculated S values for both metal-BaF_2 and metal-LiF interfaces.

TABLE IV. Energy-band parameters and dielectric constants of the ionic insulator BaF_2 and LiF.

Insulator	$\hbar\omega_p$ (eV)[c]	χ (eV)	E_w (eV)	E_g (eV)	m_I/m	$\epsilon_I(0,0)$
BaF_2[a]	20	0.2	2.9±0.2	10.5	24	7.2
LiF[b]	25	−1.8	4.6±0.3	13.6	14	9.3

[a]Band-structure parameters taken from R. T. Poole, Chem. Phys. Lett. 36, 401 (1975); W. Pong, C. S. Inouye, and S. K. Okada Phys. Rev. B 18, 4422 (1978). Dielectric constant from K. V. Rao and K. Samkula, J. Appl. Phys. 37, 319 (1966).
[b]Band-structure parameters taken from W. Pong and C. S. Inouye, J. Electron Spectrosc. Relat. Phenom. 11, 165 (1977). Dielectric constant from A. J. Dekker, *Solid State Physics* (Prentice-Hall, Englewood Cliffs, N.J., 1963), p. 145.
[c]V. A. Ganin, M. G. Karin, V. K. Sidorin, K. K. Sidorin, N. V. Starostin, G. P. Startsev, and M. P. Shepilov, Fiz. Tekh. Poluprovdn. 16, 3554 (1974) [Sov. Phys.—Solid State 16, 2313 (1975)]; D. M. Roessler and W. C. Walker, J. Phys. Chem. Solids 28, 1507 (1967).

TABLE V. Calculated values of dipole energies Δ_0 and Δ_1 and photoemission threshold ϕ_T for metals with thin BaF_2 or LiF overlayers. All energy quantities are in eV. The $\phi_T^{(\text{expt})}$ values are from Ref. 2.

Metal	ϕ_{mv}	X_m	BaF_2 Δ_0[a]	BaF_2 Δ_1	BaF_2 ϕ_T	BaF_2 $\phi_T^{(\text{expt})}$ (± 0.2 eV)	LiF Δ_1	LiF ϕ_T	LiF $\phi_T^{(\text{expt})}$ (± 0.2 eV)
Na	2.3	0.9	0.7	0.2	1.8		0.2	1.8	
Mg	3.6	1.2	1.7	0.5	2.4	2.2	0.4	2.3	1.9
Al	4.2	1.5	2.5	0.9	2.6	2.6	0.9	2.6	2.5
Cr	3.9	1.6	2.4	1.3	2.8	2.8	1.2	2.7	2.7
Cu	4.4	1.9	3.1	1.9	3.2		1.8	3.1	
Ag	4.0	1.9	2.0	1.4	3.4	3.2	1.3	3.3	3.1
Pt	5.3	2.2	5.3	3.7	3.7	3.6	3.6	3.6	3.5
Au	5.1	2.4	3.6	2.6	4.1	3.9	2.7	4.2	3.8

[a]With the exception of Mg, Al, and Au, the calculated values of Δ_0 are comparable to the values reported by J. R. Smith (Ref. 41).

V. DISCUSSION OF RESULTS

We shall consider the relation of our model to the static dipole model and in particular the implication of our results concerning the limiting value of the interface parameter for large band-gap materials.

First we wish to emphasize that our calculation of ϕ_T does not involve any assumption concerning the linear dependence of the interfacial barrier height, metal work function, and dipole energies on X_m. Thus, we determined S as the mean slope of ϕ_T vs X_m. The original derivation of the static dipole model assumed that ϕ_{mv} is linear in X_m and that D_s is essentially independent of energy in the band gap. However, we can derive the static dipole model[10] from the assumption that ϕ_B, ϕ_{mv}, Δ_0, and Δ_1 are linear functions of X_m. We can illustrate this by calculating the change in dipole energy with respect to a change in ϕ_B. From Eq. (2.23), we may write

$$\frac{\partial \phi_B}{\partial X_m}=\frac{\partial \phi_{\text{mv}}}{\partial X_m}+\frac{\partial \Delta_1}{\partial X_m}-\frac{\partial \Delta_0}{\partial X_m}\ , \tag{5.1}$$

where all partial derivatives are assumed to be independent of X_m. Using Eqs. (4.2), (4.3), (5.1), and the relationship

$$\frac{\partial(\Delta_1-\Delta_0)}{\partial X_m}=\left[\frac{\partial \phi_B}{\partial X_m}\right]\left[\frac{\partial(\Delta_1-\Delta_0)}{\partial \phi_B}\right]\ , \tag{5.2}$$

we obtain

$$S=A\left[1-\frac{\partial(\Delta_1-\Delta_0)}{\partial \phi_B}\right]^{-1}\ . \tag{5.3}$$

Comparing Eq. (5.3) with Eq. (4.4), we find

$$\frac{\partial(\Delta_1-\Delta_0)}{\partial \phi_B}=-4\pi e^2 D_s \delta_{\text{eff}}\ . \tag{5.4}$$

This quantity can also be calculated from our model. Using Eqs. (B11) and (A19), we write

$$\frac{\partial(\Delta_1-\Delta_0)}{\partial \phi_B}=\frac{\partial}{\partial \phi_B}[4\pi e^2(\eta_1\delta_{\text{eff},1}-\eta_0\delta_{\text{eff},0})]\ , \tag{5.5}$$

where

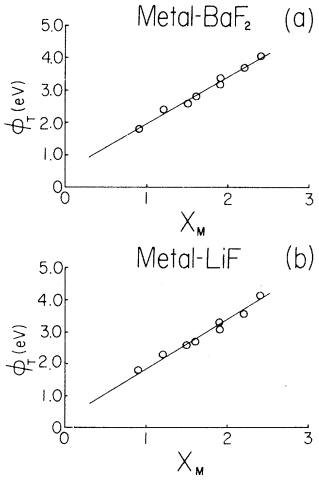

FIG. 3. Calculated photoemission threshold ϕ_T of a metal with a thin overlayer of ionic insulator vs metal electronegativity X_m. The values of X_m for the metals are listed in Table V. (a) Metals with thin BaF_2 overlayer. Calculated slope is 1.4. The measured slope is 1.4 ± 0.2. (b) Metals with thin LiF overlayer. Calculated slope is 1.5. The measured slope is 1.6 ± 0.2.

TABLE VI. Calculated values of the effective charge separation and the number of electrons transferred per unit area for metals with thin BaF_2 or LiF overlayers.

Metal	δ_m (Å)	η_0 (10^{14} cm^{-2})	BaF_2 $\delta_{\text{eff},0}$ (Å)	BaF_2 $\delta_{\text{eff},1}$ (Å)	BaF_2 η_1 (10^{14} cm^{-2})	LiF $\delta_{\text{eff},1}$ (Å)	LiF η_1 (10^{14} cm^{-2})
Na	0.63	0.3	1.13	0.77	0.15	0.76	0.14
Mg	0.46	1.2	0.86	0.60	0.47	0.59	0.45
Al	0.38	2.1	0.76	0.56	0.9	0.56	1.0
Cr	0.46	1.7	0.83	0.60	1.0	0.59	1.0
Cu	0.46	2.4	0.83	0.60	1.6	0.59	1.4
Ag	0.52	1.4	0.85	0.66	1.1	0.65	1.1
Pt	0.50	3.6	0.83	0.64	3.0	0.63	3.0
Au	0.52	2.5	0.84	0.69	2.1	0.65	2.2

$$\delta_{\text{eff},1}=\delta_m+\left[\sum_\alpha \frac{\bar{z}_{1,\alpha}\eta_{1,\alpha}}{\epsilon_I(\bar{q}_\alpha)}\right]\eta_1^{-1}, \tag{5.6}$$

$$\eta_1=\sum_\alpha \eta_{1,\alpha}, \tag{5.7}$$

$$\delta_{\text{eff},0}=\delta_m+\left[\sum_\alpha \bar{z}_{0,\alpha}\eta_{0,\alpha}\right]\eta_0^{-1}, \tag{5.8}$$

$$\eta_0=\sum_\alpha \eta_{0,\alpha}. \tag{5.9}$$

As indicated in Table VI, the variations of $\delta_{\text{eff},1}$ from metal to metal are relatively small. Hence for a given insulator we may approximate the right side of Eq. (5.5) by replacing $\delta_{\text{eff},1}$ by its mean value $\bar{\delta}_{\text{eff},1}$. Accordingly, we obtain

$$\frac{\partial(\Delta_1-\Delta_0)}{\partial\phi_B}\simeq -4\pi e^2\left[\frac{\partial}{\partial\phi_B}\left[\eta_0\frac{\delta_{\text{eff},0}}{\bar{\delta}_{\text{eff},1}}-\eta_1\right]\right]\bar{\delta}_{\text{eff},1}. \tag{5.10}$$

A comparison of Eq. (5.10) with Eq. (5.4) suggests the identification of δ_{eff} with our parameter $\bar{\delta}_{\text{eff},1}$. With this result, we can use Eqs. (4.2), (5.2), (5.4), and (5.10) to get

$$D_s=S^{-1}\left[\frac{\partial\Delta_0}{\partial X_m}-\frac{\partial\Delta_1}{\partial X_m}\right](4\pi e^2\bar{\delta}_{\text{eff},1})^{-1}. \tag{5.11}$$

Note that the determination of D_s from Eq. (5.11) is independent of an assumed value of A. Thus we can calculate the effective density of interfacial states from the calculated values of S, $\bar{\delta}_{\text{eff},1}$, $\partial\Delta_0/\partial X_m$, and $\partial\Delta_1/\partial X_m$. For metal-$BaF_2$ and metal-LiF interfaces, the values of D_s are found to be about 2×10^{13} and 1×10^{13} (cm^{2}eV)$^{-1}$, respectively. These values are somewhat smaller than Cohen's estimate of D_s for a hypothetical wide band gap material,[34] but they are of the same order of magnitude. The linear fits to $\Delta_0(X_m)$ and $\Delta_1(X_m)$ are shown in Fig. 4.

A comparison of Eq. (5.10) with Eq. (5.4) also suggests

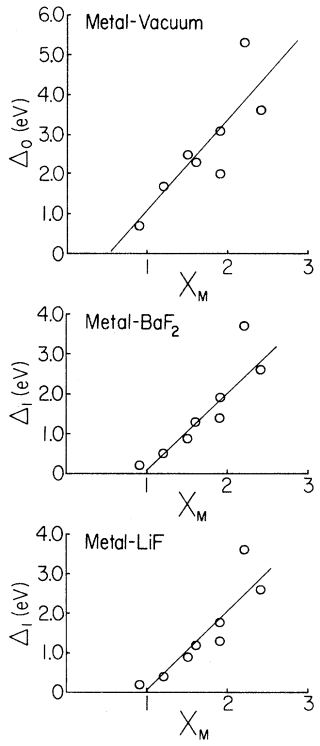

FIG. 4. Linear fits to $\Delta_0(X_m)$ and $\Delta_1(X_m)$. A slope of 2.3 is obtained from the calculated values of Δ_0 vs X_m of the metals. Slopes $\partial\Delta_1/\partial X_m$ for metal-BaF_2 and metal-LiF are found to be 2.0 and 2.1, respectively.

$$D_s \simeq \frac{\partial}{\partial \phi_B}\left[\eta_0\left[\frac{\delta_{\text{eff},0}}{\delta_{\text{eff},1}}\right]-\eta_1\right] . \tag{5.12}$$

This means that $D_s d\phi_B$ can be related to the change in number of electrons transferred per unit area across the interface. According to our calculations, the change in $(\Delta_0-\Delta_1)$ is due largely to the difference $(\eta_0-\eta_1)$ and the dielectric screening in the insulator. For metal-BaF_2 and metal-LiF interfaces with metal states fringing into the insulator, the calculations indicate that $\eta_0>\eta_1$. The values of η_0 and η_1 are shown in Table VI. The reduction of η_1 leads to a smaller Δ_1 and hence a smaller ϕ_T. Evidently, the change in ϕ_T is sensitive to the band structures of the metal *and* the ionic insulator.

Recently the limiting value of S for large band-gap materials has been a subject of considerable interest. Cohen[34] suggested that a reasonable maximum value of the band gap might be 20 eV, and using the static dipole model, he estimated the maximum value of S to be about 1.5. To check this estimate we calculated ϕ_T for metals with a thin overlayer of a hypothetical material having a band gap of 20 eV, electron affinity of 0.2 eV, and a dielectric constant of BaF_2. To double the band gap of BaF_2, we reduced the interionic separation of BaF_2 by a factor of 2. Assuming the valence-band width of the insulator is proportional to d^{-2}, where d is the nearest-neighbor distance,[35] we estimated this bandwidth to be 4 times as large as that of BaF_2. For the assumed band-parameter values, the slope $\partial\phi_T/\partial X_m$ was found to be about 1.5, in good agreement with Cohen's result. For metal-ionic insulator interfaces, we find very little change in the calculated S values for different band gaps in the range from 10 to 20 eV. We therefore expect $S\simeq 1.5$ to be, within $\pm 15\%$, a reasonable upper bound for this quantity.

VI. CONCLUSIONS

We have developed a relatively simple model of a metal-insulator interface. The model includes a multiband free-electron description of the metal, which accounts sufficiently for the band-structure and correlation effects to permit a remarkably good agreement between the calculated and measured photoemission thresholds of metals with thin overlayers of ionic insulator. We have discussed the relation of our model to the static dipole model and found the two models to give reasonably close estimates of the limiting value of the interface parameter S, the effective charge separation, and densities of interfacial states. However, in contrast to the static dipole model, our model does not depend on the uncertain value A, which occurs in the linear relation $\phi_{\text{mv}}=AX_m+B$.

The model confirms the observation that the photoemission threshold of metals covered with a thin overlayer of ionic insulator is reduced below the metal work function. Physically this is a consequence of the dielectric screening of the dipole moment associated with the charge transferred into the insulator and a reduced number of electrons transferred per unit area across the metal-insulator interface.

The calculations lend strong support to the suggestion that the interfacial dipole energies reflect charge transfers from the metal into the insulator due to the fringing of metal states into the insulator. However, we cannot totally rule out other mechanisms which may also contribute to the interfacial dipole moments.[36]

Finally, our model has the advantage of being sufficiently simple to provide a practical algorithm for the calculation of the photoemission thresholds for metals with a thin overlayer of ionic insulator. This suggests the interest in an investigation of the applicability of this simple model to metals with a thin overlayer of a covalent insulator and possibly a semiconductor.

ACKNOWLEDGMENTS

We would like to express our appreciation to Professor M. L. Cohen, Professor L. M. Falicov, Professor C. Fadley, and Professor J. Schulman for helpful discussions. One of us (T.E.F) would also like to express his appreciation for the gracious hospitality extended to him by the Physics Department of the University of Hawaii at Manoa during his visit.

APPENDIX A: CALCULATION OF Δ_0

In this appendix we outline the calculation of the dipole energy Δ_0 and the generalization to account for p- or d-band electrons having effective-mass ratio $\beta^{-1}\neq 1$.

The continuity conditions imposed on effective-mass functions lead to the following generalization of Eqs. (2.6) and (2.7):

$$T=\frac{2\beta k_z}{\beta k_z+iK} , \tag{A1}$$

$$k_z=[(2m/\hbar^2\beta)(E+E_{\alpha,1})-k_\rho^2]^{1/2}\,, \tag{A2}$$

$$K=[(2m/\hbar^2)(-E)+k_\rho^2]^{1/2}\,, \tag{A3}$$

where

$$\beta^{-1}=m_\alpha/m\,. \tag{A4}$$

Carrying out the integration with respect to z and converting the sum over occupied states n into an integration with respect to the wave vector k, we obtain the contribution of the g_α-fold degenerate α band to the first integral of Eq. (2.2). Denoting this contribution by $\mu_{0-}^{(\alpha)}$, we write

$$\mu_{0-}^{(\alpha)}=\sum_n{}' \int_{-\infty}^{0} |\Psi_n(\vec{r})|^2 z\,dz=-\frac{g_\alpha}{(2\pi)^2}\int_{-E_{\alpha,1}}^{-E_\alpha} dE\int_0^{k_{\rho,M}^2}\frac{4\beta^2k_z^2}{(\beta k_z)^2+K^2}\frac{1}{(2K)^2}\frac{dk_z}{dE}d(k_\rho^2)\,, \tag{A5}$$

where

$$k_{\rho,M}^2=(2m/\hbar^2\beta)(E_{\alpha,1}+E)\,, \tag{A6}$$

and the other quantities were defined by Eqs. (2.14)–(2.16). Performing the integration for $\beta\neq1$, we obtain

$$\mu_{0-}^{(\alpha)}=-\frac{g_\alpha}{(2\pi)^2}(1-\beta)^{-1}[(2m/\hbar^2\beta)(E_{\alpha,1}-E_\alpha)]^{1/2} \times\left[r\ln\left|\frac{1+r}{1-r}\right|-s^{-1}\ln\left|\frac{1+s}{1-s}\right|-u^{-1}\ln\left|\frac{1+u}{1-u}\right|+v\ln\left|\frac{1+v}{1-v}\right|\right], \tag{A7}$$

where

$$r=\{[E_{\alpha,1}-(1-\beta)E_\alpha](E_{\alpha,1}-E_\alpha)^{-1}\}^{1/2}\,, \tag{A8}$$

$$s=[(E_{\alpha,1}-E_\alpha)E_{\alpha,1}^{-1}]^{1/2}\,, \tag{A9}$$

$$u=r^{-1}(1-\beta^2)^{1/2}\,, \tag{A10}$$

$$v=s^{-1}(1-\beta)^{-1/2}\,. \tag{A11}$$

For s electrons and $\beta=1$, we write

$$\mu_{0-}^{(\alpha)}=-\frac{2}{(2\pi)^2}(2mE_F/\hbar^2)^{1/2}x^{1/2}\int_0^x\left[\ln\left|\frac{1+\nu^{1/2}}{1-\nu^{1/2}}\right|-2\nu^{1/2}\right]d\nu\,, \tag{A12}$$

where

$$x=E_{\rm cm}/E_F\,. \tag{A13}$$

Thus for the s electrons with $\beta=1$, we have

$$\mu_{0-}^{(\alpha)}=-\frac{1}{(2\pi)^2}k_F\left[\tfrac{1}{2}(x^{-1/2}-x^{1/2})\ln\left|\frac{1+x^{1/2}}{x^{1/2}-1}\right|+1-\tfrac{2}{3}x^{-1}\right]. \tag{A14}$$

A similar calculation has to be performed for the second integral of Eq. (2.2). Denoting this integral by $\eta_{0,\alpha}$ for a given α band and $\beta\neq1$, we find that the integration leads to

$$\eta_{0,\alpha}=\frac{g_\alpha}{(2\pi)^2}\frac{2\beta}{(1-\beta^2)}k_F^2\left[\frac{E_{\alpha,1}}{E_F}\right]\left\{\left[\frac{E_\alpha}{E_{\alpha,1}}\right]\left[\tan^{-1}\left[\frac{w}{\beta^{1/2}}\right]-\beta^{-1}\tan^{-1}(\beta^{1/2}w)\right]\right.$$

$$\left.-(1-\beta)^{-1}\left[\tan^{-1}(\beta^{1/2}w)+\tan^{-1}\left[\frac{w}{\beta^{1/2}}\right]-(\beta^{1/2}+\beta^{-1/2})\tan^{-1}w\right]\right\}, \tag{A15}$$

where

$$w=[(E_{\alpha,1}-E_\alpha)E_\alpha^{-1}]^{1/2} . \tag{A16}$$

For s electrons and $\beta=1$, we have

$$\eta_{0,\alpha}=\frac{1}{(2\pi)^2}\frac{3}{4}k_F^2[(\tfrac{4}{3}-x)\sin^{-1}(x^{-1/2})+(x-1)^{1/2}(1-\tfrac{2}{3}x^{-1})] . \tag{A17}$$

Using Eqs. (2.2), (A5), (A15), or (A17), we obtain

$$\Delta_0^{(\alpha)}=-4\pi e^2(\mu_{0-}^{(\alpha)}-\delta_m\eta_{0,\alpha}) . \tag{A18}$$

For metals with multiconduction bands, the dipole energy Δ_0 is given by

$$\Delta_0=-4\pi e^2\sum_\alpha(\mu_{0-}^{(\alpha)}-\delta_m\eta_{0,\alpha}) . \tag{A19}$$

The value of β can be calculated from Eq. (2.17) for the s and p bands that are filled up to energy E_α. We can also use Eq. (2.17) for d bands that are not completely filled. From Eq. (2.17), we find

$$\frac{m_\alpha}{m}=\left[\frac{3\pi^2N_\alpha}{g_\alpha}\right]^{2/3}\left[\frac{\hbar^2}{2m}\right](E_{\alpha,1}-E_\alpha)^{-1} . \tag{A20}$$

For the filled d bands located below the Fermi level, the effective mass of the electron is estimated using the tight-binding approximation. The highest and lowest occupied states of the filled band are assumed to be located at X and Γ, respectively. For the electrons in the filled d bands of fcc metals, the effective mass m_α is approximately

$$m_\alpha=\frac{8\hbar^2}{Ba_c^2} , \tag{A21}$$

where B is the width of the filled d band and a_c is the edge of the cubic unit cell.[37]

APPENDIX B: CALCULATION OF Δ_1

In this appendix we present the integrals representing the sums over occupied metal states in Eq. (2.24). We then discuss and derive the mean-value approximation of these integrals.

In order to find $\mu_{1-}^{(\alpha)}$, we evaluate the first integral of Eq. (2.24). Substituting Eqs. (A1)–(A4), (2.19), (2.20), and (2.28) into Eq. (2.24) with $k_I=0$, $\vec{k}_{\rho_0}=0$, and $m_I/m_\alpha=\gamma$, we obtain

$$\mu_{1-}^{(\alpha)}=\sum_n{}'\int_{-\infty}^0|\Psi_{n,\alpha}(\vec{r})|^2z\,dz=-\frac{g_\alpha}{(2\pi)^2}\int_{-E_0}^{-E_\alpha}dE\int_0^{k_{\rho,M}^2}\frac{(2\gamma k_z)^2}{[(\gamma k_z)^2+K_I^2]}\frac{1}{(2K_I)^2}\frac{dk_z}{dE}d(k_\rho^2) . \tag{B1}$$

The right-hand side of Eq. (B1) represents the contribution of the g_α-fold degenerate α band to $\mu_{1-}^{(\alpha)}$. E_0 is the smaller of the two energies E_v or $E_{\alpha,1}$. K_I is given by Eq. (2.20). The integral with respect to k_ρ^2 can be written as

$$I(E)=\frac{m\gamma^2}{\beta\hbar^2(1-\gamma^2)}\int_0^a\frac{(a-x)^{1/2}}{(b+x)(c+x)}dx , \tag{B2}$$

where

$$a=k_{\rho,M}^2=(2m/\beta\hbar^2)(E+E_{\alpha,1}) , \tag{B3}$$

$$b=(\gamma^2a+c)(1-\gamma^2)^{-1} , \tag{B4}$$

$$c=-(2m_I/\hbar^2)E_g^{-1}(E+E_v)(E+E_c) . \tag{B5}$$

Unfortunately, $I(E)$ cannot be integrated analytically with respect to E in a closed form. However, if the integral in Eq. (B2) is approximated by means of the mean-value theorem of integral calculus, then the integration indicated in Eq. (B1) can be performed analytically. Using the mean value theorem, we write

$$\int_0^a(a-x)^{1/2}(b+x)^{-1}(c+x)^{-1}dx\simeq(a-\bar{x})^{1/2}(b+\bar{x})^{-1}(c+\bar{x})^{-1}a,\quad 0<\bar{x}<a . \tag{B6}$$

The mean value of the integrand was approximated by choosing $\bar{x}=a/2$. The value was chosen because the integrand is a monotonically decreasing function of x. With this approximation we can express $\mu_{1-}^{(\alpha)}$ as

$$\mu_{1-}^{(\alpha)}=-\frac{g_\alpha 2^{-3/2}}{(2\pi)^2}(2mE_g/\hbar^2\beta)^{1/2}E_g^{3/2}\int_{U_0}^{U_u}\frac{2U^4dU}{(U_1^2-U^2)(U^2-U_2^2)(U_3^2-U^2)(U^2-U_4^2)}\ , \tag{B7}$$

where

$$2U_{1,2}^2=2E_{\alpha,1}-\left[E_v+E_c-\frac{(1+\gamma^2)}{2\gamma}E_g\right]\pm\left[\left[E_v+E_c-\frac{1+\gamma^2}{2\gamma}E_g\right]^2-4\left[E_vE_c-\frac{1+\gamma^2}{2\gamma}E_gE_{\alpha,1}\right]\right]^{1/2}\ , \tag{B8}$$

$$2U_{3,4}^2=2E_{\alpha,1}-[E_v+E_c-(2\gamma)^{-1}E_g]\pm\{[E_v+E_c-(2\gamma)^{-1}E_g]^2-4[E_vE_c-(2\gamma)^{-1}E_gE_{\alpha,1}]\}^{1/2}\ . \tag{B9}$$

U_0^2 is $(E_{\alpha,1}-E_v)$ or 0, whichever is larger, and U_u^2 is $(E_{\alpha,1}-E_\alpha)$. The mean-value approximation significantly speeds up the iterative process of solving for Δ_1.

We now evaluate the second integral of Eq. (2.24). Representing the integral by $\eta_{1,\alpha}$ and using the mean value approximation, we write

$$\eta_{1,\alpha}=\frac{2g_\alpha}{(2\pi)^2}\left[\frac{2mE_g}{\hbar^2}\right]\left[\frac{2m_IE_g}{m\beta}\right]^{1/2}\int_{U_0}^{U_u}\frac{U^4[(U_3^2-U^2)(U^2-U_4^2)]^{-1/2}}{(U_1^2-U^2)(U^2-U_2^2)}dU\ . \tag{B10}$$

A partial fraction expansion reduces the integral to a linear combination of elliptic integrals[38,39] of the first and third kind. These integrals are tabulated functions.[40]

The dipole energy Δ_1 can be determined from

$$\Delta_1=-4\pi e^2\sum_\alpha\left[\frac{\mu_{1-}^{(\alpha)}}{\epsilon_I(\bar{q}_\alpha)}-\delta_m\eta_{1,\alpha}\right]\ . \tag{B11}$$

Here it should be recalled that all the energies $(E_{\alpha,1},E_\alpha,\phi_{\rm mv})$ characterizing the metal have to be referred to the vacuum level of the insulator rather than that of the metal. That is, they have to include an additive term $(\Delta_1-\Delta_0)$. Thus both the integrands and the limits of integration in Eqs. (B7) and (B10) contain an explicit dependence on the unknown dipole energy Δ_1.

The effective mass m_I of the electron in the insulator is calculated using the reported values of the valence-band width E_w and the plasmon energy $\hbar\omega_p$. Applying Eq. (A20) to the F^- $2p$ band of the insulator and using the expression

$$\omega_p=(4\pi e^2N_v/m_I)^{1/2}\ , \tag{B12}$$

where N_v is the effective number of valence-band electrons per unit volume in the insulator, we find

$$m_I=(\hbar\omega_p)^4(\pi\hbar)^2/128E_w^3e^4\ . \tag{B13}$$

*Visitor at the University of Hawaii at Manoa. Permanent address: Department of Physics, Pennsylvania State University, University Park, PA 16802.

[1]S. Kurtin, T. C. McGill, and C. A. Mead, Phys. Rev. Lett. 22, 1433 (1969).
[2]W. Pong and D. Paudyal, Phys. Rev. B 23, 3085 (1981).
[3]J. Bardeen, Phys. Rev. 71, 717 (1947).
[4]V. Heine, Phys. Rev. 138, A1689 (1965).
[5]A. J. Bennett and C. B. Duke, Phys. Rev. 162, 578 (1967).
[6]J. C. Phillips, Phys. Rev. B 1, 593 (1970).
[7]J. C. Inkson, J. Phys. C 5, 2599 (1972).
[8]S. G. Louie and M. L. Cohen, Phys. Rev. Lett. 35, 866 (1975).
[9]C. Tejedor, F. Flores, and E. Louis, J. Phys. C 10, 2163 (1977).
[10]S. G. Louie, J. R. Chelikowsky, and M. L. Cohen, J. Vac. Sci. Technol. 13, 790 (1976).
[11]L. J. Brillson, J. Vac. Sci. Technol. 16, 1137 (1979).
[12]W. E. Spicer, I. Lindau, P. Skeath, C. Y. Su, and P. Chye, Phys. Rev. Lett. 44, 420 (1980).
[13]I. Lindau, P. W. Chye, C. M. Garner, P. Pianetta, C. Y. Su, and W. E. Spicer, J. Vac. Sci. Technol. 15,

1332 (1978).
[14]Recently such a model has been successfully applied by I. Ihm, M. L. Cohen, and S. F. Tuan [Phys. Rev. B 23, 3258 (1981)] in their discussion of demons and superconductivity.
[15]The model is an adaptation of the Franz interpolation formula (Ref. 16) rather than of the inapplicable model of narrow-gap semiconductors due to Heine (Ref. 4) and developed by Garcia-Moliner and Flores (Ref. 17).
[16]W. Franz, in *Handbook of Physics,* edited by H. Geigerand K. Scheel (Springer, Berlin, 1956), Vol. 17, p. 165.
[17]F. Garcia-Moliner and F. Flores, *Introduction to the Theory of Solid Surfaces* (Cambridge University Press, New York, 1979).
[18]C. Kittel, *Quantum Theory of Solids* (Wiley, New York, 1963), p. 106.
[19](a) S. Lindhard, K. Dan. Vidensk. Selsk. Mat. Fys. Medd. 28, (1954); (b) C. Kittel, *Quantum Theory of Solids* (Wiley, New York, 1963), p. 113.
[20](a) J. Friedel, Nuovo Cimento B 7, Suppl., 287 (1958); (b) N. D. Lang, in *Solid State Physics,* edited by H. Ehrenreich, F. Seitz, and D. Turnbull (Academic, New York, 1973), Vol. 28, p. 225.
[21]This result is intuitively expected from Lang's discussion of the charge deficiency at the jellium vacuum interface [Ref. 20(b)]. This deficiency is screened within $z_s \sim \pi/2k_F$. A reasonable estimate of z_m is $z_s/2$. A formal proof follows from the analysis of the asymptotic response of the jellium to an externally imposed charge deficiency.
[22]G. E. Pake, *Paramagnetic Resonance* (Benjamin, New York, 1962), pp. 55—58.
[23]T. E. Feuchtwang and P. H. Cutler, Phys. Rev. B 14, 5237 (1976).
[24]The complex band structure is clearly discussed in Ref. 17.
[25]While we have not explicitly stated that we are developing an effective-mass-type theory for the interface, this is in fact implict in the nonclassical dispersion relations involving effective masses such as specified by Eqs. (2.17) and (2.20). Such theories have been discussed in detail in Ref. 26.
[26]C. B. Duke, *Tunneling in Solids, Solid State Physics* (Academic, New York, 1969), Suppl. 10.
[27]A more detailed discussion of these states is given by S. G. Louie and M. L. Cohen, Phys. Rev. B 13, 2461 (1976).
[28]Note that this definition differs from that proposed by Louie *et al.* in Ref. 10.
[29]J. P. Walter and M. L. Cohen, Phys. Rev. B 2, 1821 (1970).
[30]D. R. Penn, Phys. Rev. 128, 2093 (1962).
[31]For a discussion of this empirical relation, see Ref. 32.
[32]W. Gordy and W. J. D. Thomas, J. Chem. Phys. 24, 439 (1956).
[33]M. Schlüter, Phys. Rev. B 17, 5044 (1978).
[34]M. L. Cohen, J. Vac. Sci. Technol. 16, 1135 (1979).
[35]W. A. Harrison, *Electronic Structure and the Properties of Solids* (Freeman, San Francisco, 1980), p. 323.
[36]A. Zunger, Phys. Rev. B 24, 4372 (1981).
[37]C. Kittel, *Introduction to Solid State Physics,* 5th ed. (Wiley, New York, 1976), p. 263.
[38]See, for example, *Handbook of Mathematical Functions,* edited by M. Abramowitz and I. A. Stegun (U.S. Government Printing Office, Washington, D.C., 1964).
[39]I. S. Gradshteyn and I. M. Ryzhik, *Table of Integrals Series and Products* (Academic, New York, 1965).
[40]H. E. Fettis and J. C. Caslin, *Table of the Elliptic Integrals of the First, Second, and Third Kind* (Aerospace Research Laboratories, Office of Aerospace Research United States Air Force, Wright Patterson Air Force Base, Ohio, 1964).
[41]J. R. Smith, Phys. Rev. 181, 522 (1969).